ADVANCES IN ATMOSPHERIC SCIENCES, VOL. 30, NO. 6, 2013, 1621–1631

A Global Ocean Reanalysis Product in the China Ocean Reanalysis (CORA) Project

HAN Guijun* (韩桂军), FU Hongli (付红丽), ZHANG Xuefeng (张学峰), LI Wei (李 威), WU Xinrong (吴新荣), WANG Xidong (王喜冬), and ZHANG Lianxin (张连新)

Key Laboratory of Marine Environmental Information Technology, State Oceanic Administration, National Marine Data and Information Service, Tianjin 300171

(Received 13 August 2012; revised 30 January 2013; accepted 6 February 2013)

ABSTRACT

The first version of a global ocean reanalysis over multiple decades (1979–2008) has been completed by the National Marine Data and Information Service within the China Ocean Reanalysis (CORA) project. The global ocean model employed is based upon the ocean general circulation model of the Massachusetts Institute of Technology. A sequential data assimilation scheme within the framework of 3D variational (3DVar) analysis, called multi-grid 3DVar, is implemented in 3D space for retrieving multiple-scale observational information. Assimilated oceanic observations include sea level anomalies (SLAs) from multi-altimeters, sea surface temperatures (SSTs) from remote sensing satellites, and *in-situ* temperature/salinity profiles.

Evaluation showed that compared to the model simulation, the annual mean heat content of the global reanalysis is significantly approaching that of World Ocean Atlas 2009 (WOA09) data. The quality of the global temperature climatology was found to be comparable with the product of Simple Ocean Data Assimilation (SODA), and the major ENSO events were reconstructed. The global and Atlantic meridional overturning circulations showed some similarity as SODA, although significant differences were found to exist. The analysis of temperature and salinity in the current version has relatively larger errors at high latitudes and improvements are ongoing in an updated version. CORA was found to provide a simulation of the subsurface current in the equatorial Pacific with a correlation coefficient beyond about 0.6 compared with the Tropical Atmosphere Ocean (TAO) mooring data. The mean difference of SLAs between altimetry data and CORA was less than 0.1 m in most years.

Key words: global ocean, ocean reanalysis dataset, China Ocean Reanalysis (CORA), multi-grid 3DVar

Citation: Han, G. J. , H. L. Fu, X. F. Zhang, W. Li, X. R. Wu, X. D. Wang, and L. X. Zhang, 2013: A global ocean reanalysis product in the China Ocean Reanalysis (CORA) project. *Adv. Atmos. Sci.*, **30**(6), 1621–1631, doi: 10.1007/s00376-013-2198-9.

1. Introduction

Owing to the existence of model errors, oceanic states simulated by ocean models are always different from the real world in both climatological features and variability. Ocean data assimilation (ODA) combines model dynamics with observational information to reconstruct historical and present oceanic states. The continuous time series of oceanic states that have a 3D structure on a regular mesh system is a very important source of data for better understanding the mechanisms of the varying of ocean flows through a range of diagnostics. For example, the physical relationships among different oceanic variables and the interaction mechanisms of different scale oceanic circulations could be clarified by time series analysis of related quantities. The reconstruction of present oceanic states also helps to establish initial conditions for ocean forecasting.

Worldwide efforts are ongoing to produce global ocean reanalysis datasets, and two examples of such projects are ECCO (Estimating the Circulation and Climate of the Ocean) (Stammer and Chassignet, 2000) and SODA (Simple Ocean Data Assimilation) (Carton et al., 2000a, b). Following on from earlier work reporting a regional ocean reanalysis for the

*Corresponding author: HAN Guijun, gjhan@mail.nmdis.gov.cn

coastal waters of China and adjacent seas (Han et al., 2011), developed by the Key Lab of Marine Environmental Information Technology (MEIT), this paper describes the first version of a global ocean reanalysis under the China Ocean Reanalysis (CORA; www.cora.net.cn) project, established at the National Marine Data and Information Service (NMDIS). We expect that this first version will not only provide a dataset that characterizes global oceanic circulations, but also open a door for the Chinese ocean science research community to focus on producing its own ocean reanalysis products for the global ocean as well, which are of critical importance for improving operational ocean forecasting skills.

Details of the global reanalysis system are given in section 2, including a description of the ocean model, the ocean data assimilation algorithms, as well as observational data. In section 3 we present results from an evaluation of the global reanalysis fields. And finally, in section 4, we discuss and summarize the overall findings.

2. Methodology

2.1 *Model and assimilation method*

The oceanic model used in the global ocean reanalysis system is the Massachusetts Institute of Technology General Circulation Model (MITgcm) (Marshall et al., 1997). The main characteristic of this model is that one hydrodynamical kernel can be used to drive forward both atmospheric and oceanic models (although it is used here only for an oceanic model).

The model domain in the reanalysis system covers the global ocean from 74.25°S to 84.75°N. The vertical mixing scheme adopted is the K-profile parameterization (KPP) (Large et al., 1994; Dursku et al., 2004). A horizontal C-grid has a $0.5°\times0.5°$ horizontal resolution telescoping to 0.25° meridional spacing in the tropical region, and the total horizontal grid number is 720×348. The z-level standard vertical grid is used, with a total of 35 vertical levels for configuration. The minimum and maximum water depth is 5 m and 5500 m, respectively. The time step for model integration is 600 seconds.

For the period 1 July 1987 to 31 December 2008, the wind field employed is a daily mean wind field from the new Cross-Calibrated Multi-Platform (CCMP) ocean surface wind product (Atlas et al., 2011) from the Physical Oceanography Distributed Active Archive Center (PODAAC; http://podaac.jpl.nasa.gov/DATA_CATALOG/ccmpinfo.html), with a horizontal resolution of $0.25°\times0.25°$. For the rest of the analysis period, the wind field is obtained from the US National Centers of Environmental Prediction (NCEP) reanalysis, with a spatial resolution of $1.875°\times1.875°$ and temporal resolution of 6 hours. Wind speed is converted to wind stresses using the formula of Yelland and Taylor (1996). The other atmospheric forcings, such as heat and water flux, are also taken from the NCEP reanalysis. River runoff is not considered for now.

The ocean data assimilation algorithms implemented in this global ocean reanalysis system are the same as in the regional ocean reanalysis for the coastal waters of China and adjacent seas in CORA (Han et al., 2011); namely, the kernel of a 3D variational (3DVar) analysis scheme designed within a multi-grid framework (Li et al., 2008, 2010; Xie et al., 2011). Different from traditional 3DVar performed at each model level with vertical correlations ignored (Derber and Rosati, 1989), this sequential 3DVar scheme can be performed across the entire 3D space to retrieve multi-scale information resolved by an observing system, yielding multi-scale, inhomogeneous analysis.

Details regarding the implementation of the multi-grid 3DVar can be found in Han et al. (2011). Here, we only give a brief summary of the ocean data assimilation scheme and its practical strategies used for assimilating oceanic observations:

(1) The standard 3DVar cost functional is used in the multi-grid 3DVar, but the background and observational terms operate on the field of temperature correction instead of the temperature itself (Derber and Rosati, 1989). The cost function is first minimized on coarse grids to obtain smooth modes (long-wave information), and then the grid resolution increases so that the minimized cost function retrieves oscillatory modes (short-wave information). The final adjustment of an analysis field is the sum of adjustments as the grid is refined from coarse to fine, and the newly added observations relative to the background are in turn subjected to 3DVar analysis.

(2) The salinity adjustment scheme proposed by Troccoli et al. (2002) is employed.

(3) A 3DVar scheme (Yan et al., 2004; Zhu and Yan, 2006; Zhu et al., 2006; Xiao et al., 2006, 2008; Shu et al., 2009, 2011; Wang et al., 2012a, b) is adapted He et al. (2010) to convert altimetry sea level anomalies (SLAs) data into temperature and salinity "pseudo observations" for each single water column.

(4) The assimilation is performed every seven days, and a seven-day time window was designed to incorporate SLAs from altimeters, sea surface temperatures (SSTs) from remote sensing satellites, and in-situ temperature and salinity profiles (above 2000 m) into the model.

Table 1. Data types and sources used in CORA.

Data type	Variable	Source
Ocean observations	Temperature and salinity profiles	NMDIS archive, World Ocean Database 2009 (WOD09), Global Temperature and Salinity Profile Project (GTSPP), and Argo project.
	Satellite remote sensing SST	Reynolds SST dataset (Reynolds et al., 2007) with 0.25°×0.25° and daily mean.
	SLA	Multi-satellite altimeter merged gridded product including TOPEX /POSEIDON (T/P), Jason-1, ERS-2 and Envisat (http://www.jason.oceanobs.com) with 0.25°×0.25° and 7-day mean.
Atmospheric forcing	Wind, heat and freshwater flux	NCEP reanalysis with 1.875° × 1.875° spatial resolution and 6-hour temporal resolution. The new Cross-Calibrated, Multi-Platform (CCMP) ocean surface wind from PO.DAAC with 0.25°×0.25° spatial resolution and 6-hour temporal resolution.
Initial conditions	Monthly mean temperature and salinity climatology	World Ocean Atlas 2009 (WOA09)
Water depth	Gridded water depth	ETOPO5

2.2 *Observational data*

The observational data used in this global ocean reanalysis comprise *in-situ* temperature/salinity profiles, SLAs from altimeters, and SSTs from remote sensing satellites (see Table 1 for details). A great deal of effort was devoted to ensuring the quality of the reanalysis by conducting pre-assimilation quality control of the data. For example, the temperature and salinity profiles were subjected to unified quality control, including position/time checks, depth duplication checks, depth inversion checks, temperature and salinity range checks, excessive gradient checks, and stratification stability checks. It is also worth mentioning that the drifting errors that occur to salinity profiles in Argo (Array for Real-time Geostrophic Oceanography) were corrected by using the calibration method of Wong et al. (2003).

3. Evaluation of reanalysis results

Owing to weak vertical mixing at high latitudes in the assimilation model [research indicates that vertical mixing is actually very strong in these areas (Wei et al., 2012, personal communication)], the model sensitivity was found to be too strong in assimilating data at high latitudes. Therefore, ocean data assimilation was limited to within 40°S–60°N. However, now this issue has been identified, and the vertical mixing has been strengthened, the ongoing updated version will not limit the data assimilation domain.

A 4-yr spin up of the analysis procedure was carried out, in which the model was started from January 1975 using observational temperature and salinity climatology as the initial conditions, and oceanic observations were assimilated into the model. With January 1979 as the beginning, the global ocean reanalysis dataset, also called CORA (China Ocean Reanalysis), consists of 3D oceanic states of sea surface height, 3D temperature, salinity, and currents, has been established to cover a period of 30 years from January 1979 to December 2008. It contains daily-mean fields of ocean states at the model grids. Considering the confined domain within which ocean data assimilation was performed, we only evaluated the assimilation quality in that domain.

3.1 *Annual mean and seasonal cycle*

First, we assess the time mean errors of ocean temperature and salinity of CORA using World Ocean Atlas 2009 (WOA09) data. Figure 1 shows that compared to the model simulation, the data constraints by ocean data assimilation (ODA) significantly reduced the errors of the upper ocean (0–300 m) temperature in the three basins (i.e., Indian, Pacific, and Atlantic). It was found although the ODA can reduce the errors of ocean salinity for most basins, the salinity data constraint is more difficult than that of temperature. For example, the North Atlantic became fresher through the ODA, while the Southern Ocean became saltier. Further examination showed that the salinity errors mainly came from the pre-Argo period for which salinity observations are very sparse. When salinity observations are lacking, the observational constraint of salinity completely depends upon the Temperature-Salinity (T-S) relationship that is derived from the model background. Thus, larger salinity reanalysis errors were derived from the biased T-S relationship due to model background errors.

We also examined the zonal averaged root mean square errors (RMSEs) of temperature and salinity in CORA compared to the WOA09 data, as shown in Fig. 2. Consistent with the findings from Fig. 1, Fig. 2 shows that the zonal averaged RMSEs for both temperature and salinity of the CORA reanalysis were

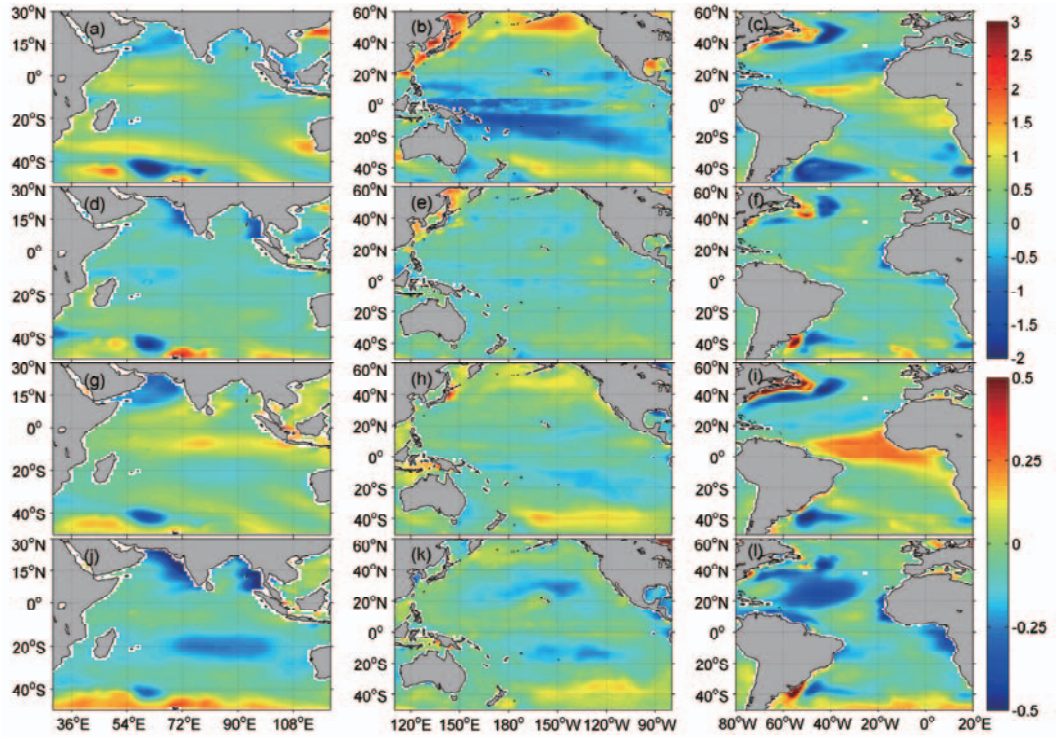

Fig. 1. Averaged errors of upper ocean (0–300 m) temperature (units: °C; a–f) and salinity (units: psu; g–l) for the Indian (a, d, g, and j), Pacific (b, e, h, and k) and Atlantic (c, f, i, and l) basins in the assimilation domain: from the model simulation (a–c and g–i) and from CORA (d–f and j–l).

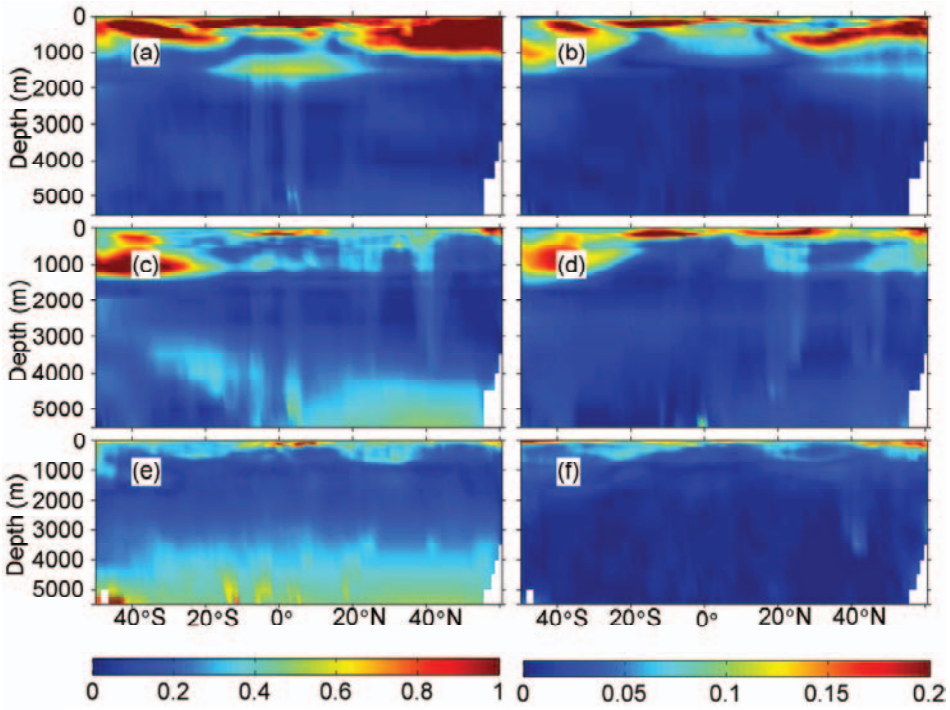

Fig. 2. Zonal averaged RMSEs of ocean temperature (units: °C; a, c, and e) and salinity (units: psu; b, d, and f) produced by the free model simulation (a and b), CORA (c and d) and SODA (e and f).

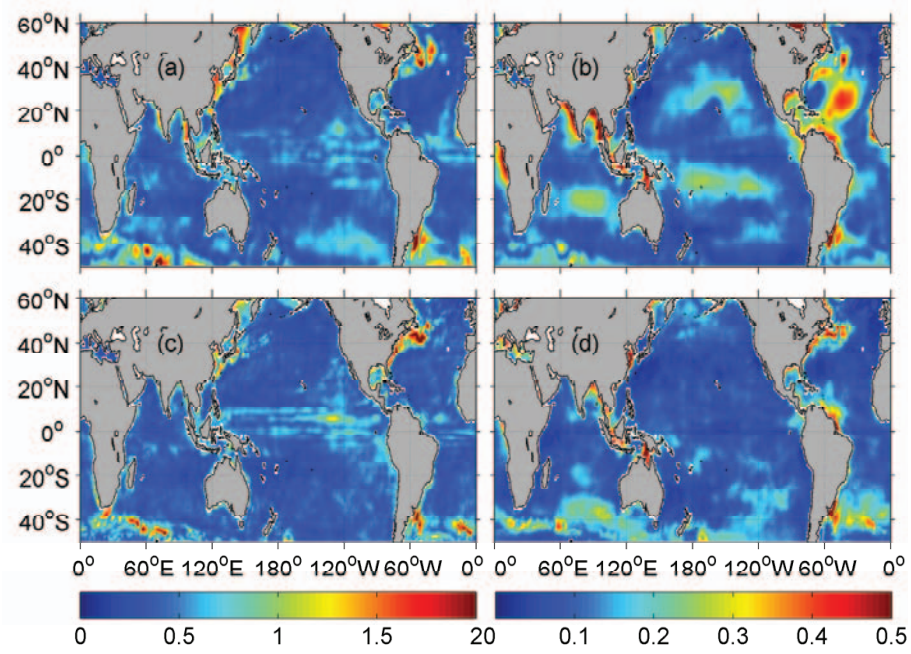

Fig. 3. Averaged RMSEs of upper ocean (0–300 m) temperature (units: °C; a and c) and salinity (units: psu; b and d) in CORA (a and b) and SODA (c and d).

much smaller than the model simulation. Except for the areas around 40°S, the CORA reanalysis showed comparable quality with SODA (versions 2.0.2 and 2.0.4) reanalysis. The relatively larger errors around 40°S could be attributed to the problem of data constraints in the area of the Antarctic Circumpolar Current, which is associated with weak vertical mixing in this version of the assimilation model, as described above. We also observed that CORA temperature errors in the deep ocean were noticeably smaller than that of SODA, probably because of the strong subsurface data constraints in CORA. Figure 3 presents the 0–300 m averaged temperature and salinity RMSEs, which also supports the conclusion that the CORA temperature quality is overall comparable with SODA in the upper ocean, and that the CORA salinity error is larger than SODA's, especially in the North Atlantic basin.

Figure 4 presents the seasonal cycle of Niño 3.4 domain-averaged temperature (Figs. 4a, c, and e) and salinity (Figs. 4b, d, and f) anomalies in the WOA09 data (Figs. 4a and b), the CORA reanalysis (Figs. 4c and d) and SODA reanalysis (Figs. 4e and f). From Fig. 4, we see that the CORA reanalysis produced a slightly better seasonal cycle simulation than SODA in the central tropical Pacific.

3.2 *Ocean heat content and ENSO variability*

Figure 5 presents the monthly mean heat content anomalies averaged over the upper ocean (0–300 m) in the three basins. While the CORA and SODA reanalyses shared overall similar variability in the basins, differences for some individual basins were found to exist. Generally speaking, the difference between CORA and SODA in the Atlantic was larger than the Pacific and Indian, and the difference at low latitudes was smaller than at high latitudes. For example, the CORA reanalysis (black line) and SODA reanalysis (red line) in Figs. 5b and c (for the tropical Pacific) are almost identical, while the difference between the two reanalyses becomes more noticeable in Figs. 5e, f, and g when the latitudes of the basin becomes higher. Compared to Figs. 5a, b, and c, the black line in Fig. 5d (tropical Atlantic) is more distinguishable from the red line. In addition, in the North Atlantic (Figs. 5h and i), the CORA reanalysis showed a large difference from the SODA reanalysis in some periods (1994–99 in Fig. 5h and 2000–04 in Fig. 5i, for instance).

Figure 6 shows the first (Figs. 6a and c) and second (Figs. 6b and d) modes of Empirical Orthogonal Function (EOF) of tropical Pacific SSTs derived from the CORA (Figs. 6a and b) and SODA (Figs. 6a and d) reanalyses. The corresponding time series of the first principle component (PC1) and second principle component (PC2) are plotted in Fig. 7. From Fig. 6, we see that both the CORA and SODA reanalyses reconstructed the first (eastern Pacific warm anomaly) and second (central Pacific warm anomaly) types of ENSO patterns very well. However, although both reanalyses shared generally the same EOF patterns, the details of

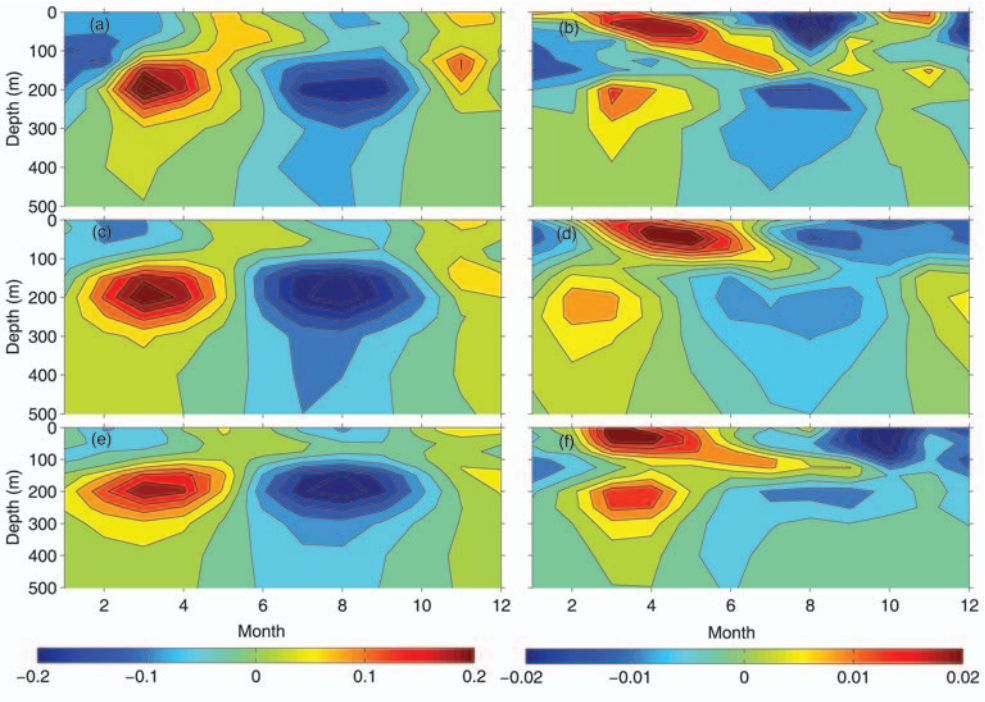

Fig. 4. Seasonal cycle of Niño 3.4 (170°–120°W, 5°S–5°N) mean temperature (units: °C; a, c, and e) and salinity (units: psu; b, d, and f) anomalies in WOA09 (a and b), CORA (c and d) and SODA (e and f).

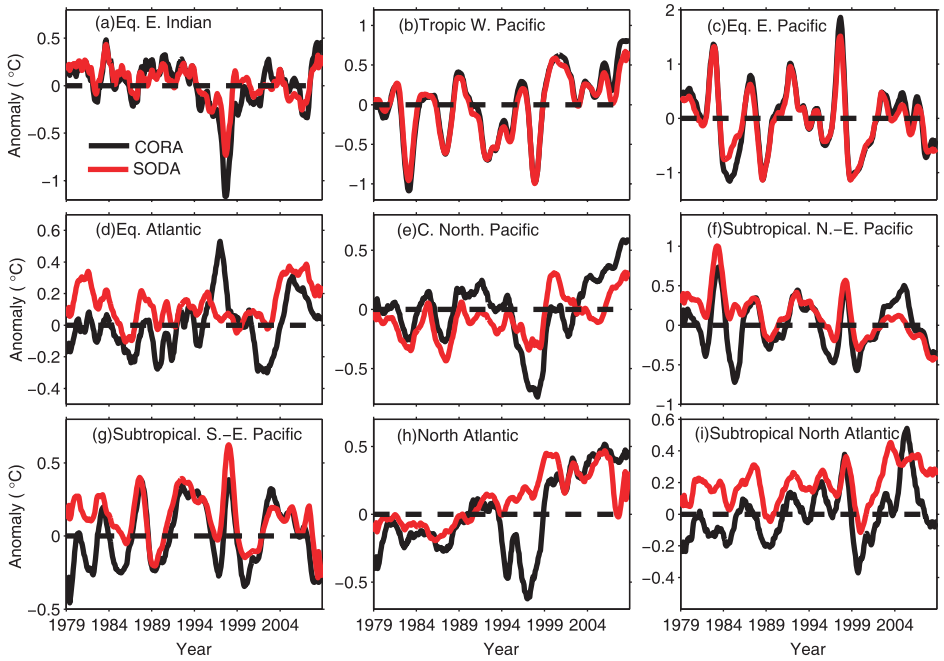

Fig. 5. Time series of upper ocean (0–300 m) heat content anomalies with 1-yr running mean in different basins in CORA (black line) and SODA (red line). (a) Equatorial eastern Indian Ocean (70°–100°E, 5°S–5°N); (b) tropical western Pacific Ocean (130°E–170°W, 20°S–20°N); (c) equatorial eastern Pacific Ocean (150°–90°W, 5°S–5°N); (d) equatorial Atlantic Ocean (50°W–10°E, 10°S–10°N); (e) central North Pacific Ocean (180°–140°W, 20°–40°N); (f) subtropical northeast Pacific Ocean (140°–90°W, 5°–25°N); (g) subtropical southeast Pacific Ocean (140°–80°W, 5°–25°S); (h) subpolar North Atlantic Ocean (80°–10°W, 30°–60°N); (i) subtropical North Atlantic Ocean (80°W–0°, 5°–25°N).

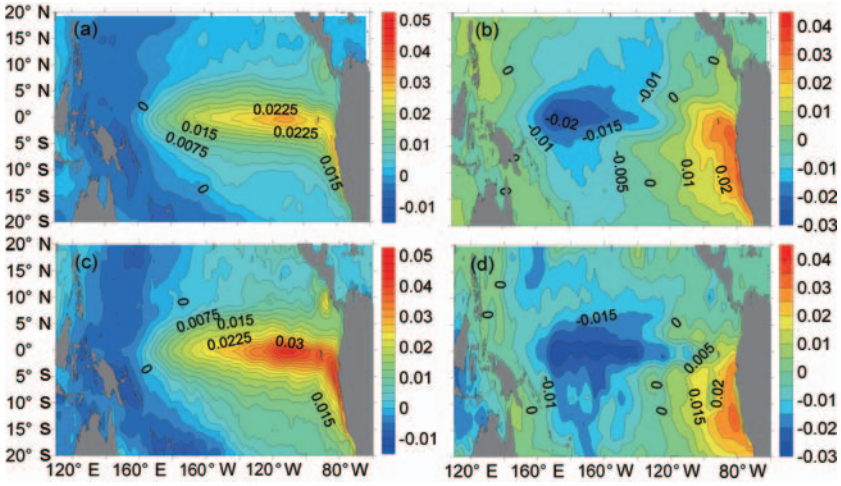

Fig. 6. First (a and c) and second (b and d) modes of EOF for tropical Pacific SSTs produced by CORA (a and b) and SODA (c and d).

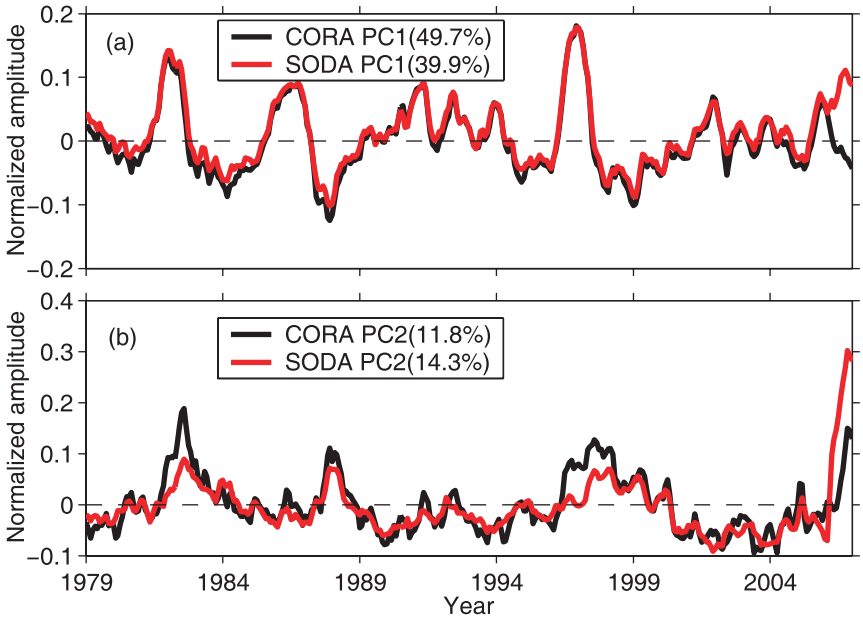

Fig. 7. Time series of the first principle component (PC1; a) and the second principle component (PC2; b) modes of EOF for tropical Pacific SSTs produced by CORA (black line) and SODA (red line).

their pattern structures were different: while the tropical instability wave structure can be observed in the SODA reanalysis, the CORA reanalysis shows a very smooth distribution. The time series of PC1 (Fig. 7a) and PC2 (Fig. 7b) provide evidence that both reanalyses retrieve the major historical ENSO events very well for both types.

3.3 *Global and Atlantic meridional overturning circulations*

Meridional overturning circulation (MOC) represents the meridional transport of water mass and can be used to characterize the general features of balance and consistency in a global ocean reanalysis. Although no complete observation is available for verification, by comparing the time mean feature and variability of the global MOC and Atlantic MOC (AMOC) in different reanalysis products, we can still achieve a good understanding of the advantages and disadvantages of a reanalysis product. Figure 8 presents the time mean global (Figs. 8a and c) and Atlantic (Figs. 8b and d) MOC obtained from the CORA (Figs. 8a and b) and SODA (Figs. 8c and d) reanalyses. As can be seen, these two reanalyses produced a very similar time

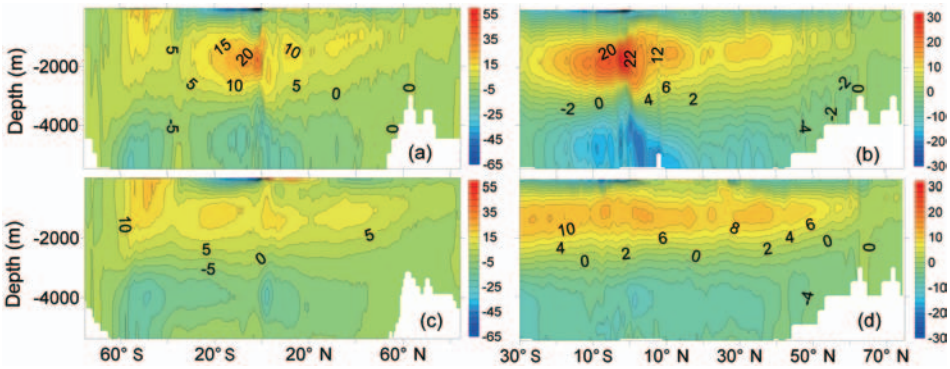

Fig. 8. Time mean of the global (a and c) and Atlantic (b and d) MOCs (units: Sv) in CORA (a and b) and SODA (c and d).

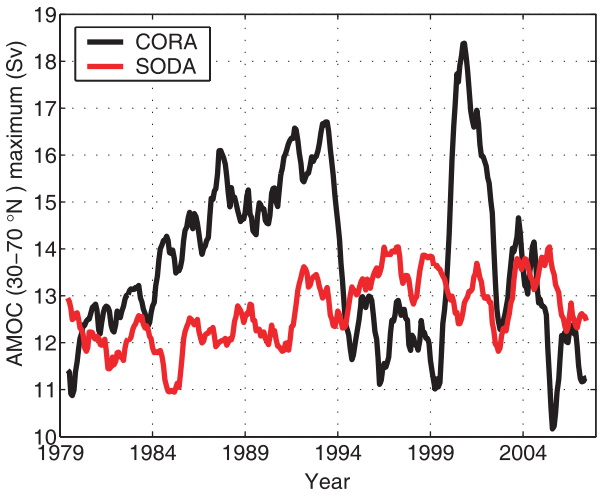

Fig. 9. Time series of the AMOC maximum (units: Sv) between 30°–70°N with 1-year running mean in CORA (black line) and SODA (red line).

mean feature for both global and Atlantic MOCs, but the variability of AMOC was quite different in CORA and SODA (see Fig. 9). Although there is no evidence to indicate which variability had the better representation, the AMOC variability in CORA appeared stronger than in SODA, and its maximum was closer to some observational estimates (Dong et al., 2009). Those differences must be associated with different mixing and overflow schemes in the assimilation models, as well as different assimilation strategies in these reanalysis systems. For example, the analysis of CORA is carried out within the latitude region of 40°S–60°N and at a depth range of 0–2000 m, but the analysis of SODA (Carton and Giese, 2008) is carried out within the latitude region of 90°S–90°N and at a depth range of 0–1000 m; CORA uses the MITgcm as the assimilation model and SODA uses the Parallel Ocean Program (POP). Obviously, plenty of research and development work is needed to further clarify the mechanisms of different overturning features and variability.

3.4 *Equatorial Pacific current and SLA*

We used equatorial TAO (Tropical Atmosphere Ocean) mooring data to validate the subsurface currents of CORA at 165°E, 170°W, 140°W and 110°W, and AVISO (Archiving Validation and Interpretation of Satellite Oceanographic) altimetry data to validate SLAs of CORA in the equatorial Pacific region, respectively.

3.4.1 *Comparison with TAO current profiles*

Figure 10 shows that the departure of zonal daily velocity in CORA from TAO as a function of depth and time at four sites of the TAO array. The correlation coefficients and RMSEs between CORA and TAO were calculated using the zonal velocity time series with 30-day running mean. Their vertical structures are also presented in Fig. 10. CORA revealed an overall negative current compared to TAO at depths below 150 m, indicating that CORA simulates a weak Equatorial Under Current (EUC). The currents of CORA at depths above 100 m at 110°W were smaller than TAO, indicating that CORA simulates a strong South Equatorial Current (SEC).

The vertical changes in correlation coefficients at all sites were not significant, and their vertical averages were larger than about 0.6. The RMSEs near the thermocline at 110°W and 140°W reached maximal values, and those at the other two sites changed very little with depth. The vertical averaged RMSEs at all sites except 110°W were less than 0.4 m s^{-1}. The vertical averaged RMSE at 110°W was largest. The reason for such a case is that the model simulations of the current at 110°W (Fig. 10a) fluctuated largely above 100 m depth compared with the other three sites, meaning the model's performance needs to

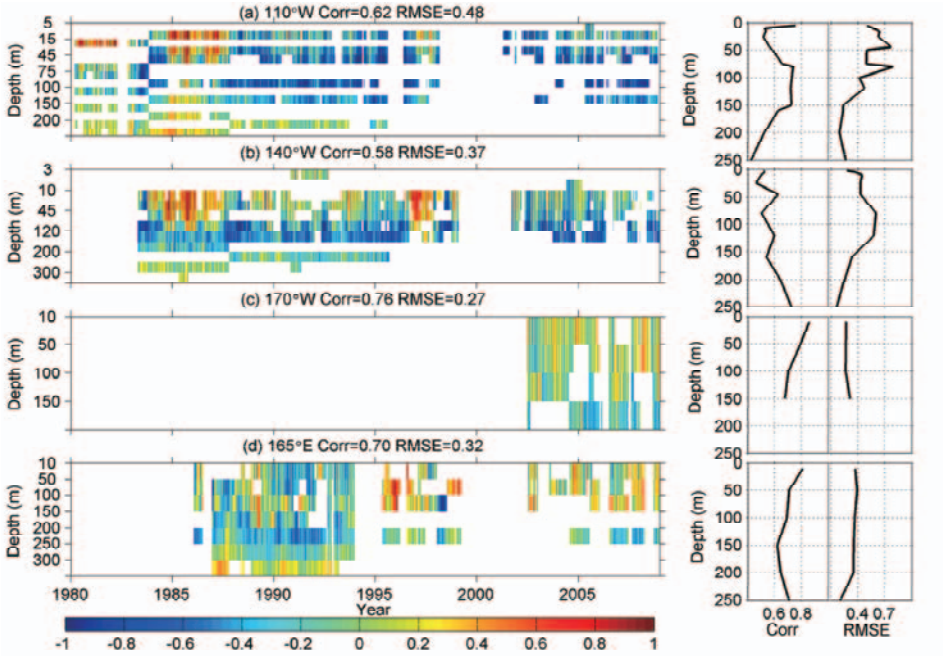

Fig. 10. Difference of zonal velocity (units: m s^{-1}) between CORA and TAO at four equatorial mooring sites: (a) 110°W, (b) 140°W, (c) 170°W, and (d) 165°E. Right two panels show the vertical structures of the correlation coefficients and RMSEs. Corr = correlation.

be improved to handle the complicated physical processes in this area. We also expect that more detailed analyses will be carried out in separate studies focusing on the variability of the equatorial current.

3.4.2 *Comparison with AVSIO altimetry data*

The SLAs of CORA averaged for 2°S–2°N in the equatorial Pacific during 1994–2008 were compared to AVISO altimetry data, and the results are presented in Fig. 11. As can be seen, the temporal pattern of CORA SLAs in the equatorial Pacific belt was very similar to those of altimetry data, and the difference between them in most years was less than 0.1 m. The CORA SLAs before 1998 were larger than in the altimetry data, and became smaller after 2000, the difference reaching −0.2 m near the year 2003. Such a change may be related to a version change of SST data assimilated into CORA, i.e., the AVHRR (Advanced Very High Resolution Radiometer) -only product version 1 from November 1981 through May 2002, and the AMSR (Advanced Microwave Scanning Radiometer) + AVHRR product version 2 from June 2002 onward; further studies are needed.

4. Discussion and summary

The first version of a global ocean reanalysis product over multiple decades has been completed by the NMDIS within the CORA project. All available satellite and in-situ observations since the end of the 1970s were assimilated into a global ocean model to produce the time series of global ocean state estimates through a multi-grid 3DVar approach.

The annual mean heat content of the global reanalysis was found to be significantly approaching that of World Ocean Atlas 2009 data, compared to the model simulation. The quality of the global temperature climatology is comparable with the product of SODA, while the salinity error is larger than that of SODA owing to different model performances with sparse salinity observations. The major events of ENSO were found to be reconstructed very well, as with SODA. The time mean of global and Atlantic MOCs showed similar features as the SODA product, but significant differences were found to exist in the variability of the AMOC. The EUC in the equatorial Pacific was weak, and the SEC in the eastern Pacific strong compared to TAO mooring data, but their correlation coefficients were beyond about 0.6. The difference of equatorial SLAs between CORA and AVISO altimetry data was found to be small in all years except 2003, which could be attributed to a version change of the assimilated SST data. The current version has relatively larger errors at high latitudes, and improvements are ongoing in an updated version. In addition, in a test experiment with the updated version, the salinity analysis errors have been relaxed by the improvement in the model that provides a better background T-S rela-

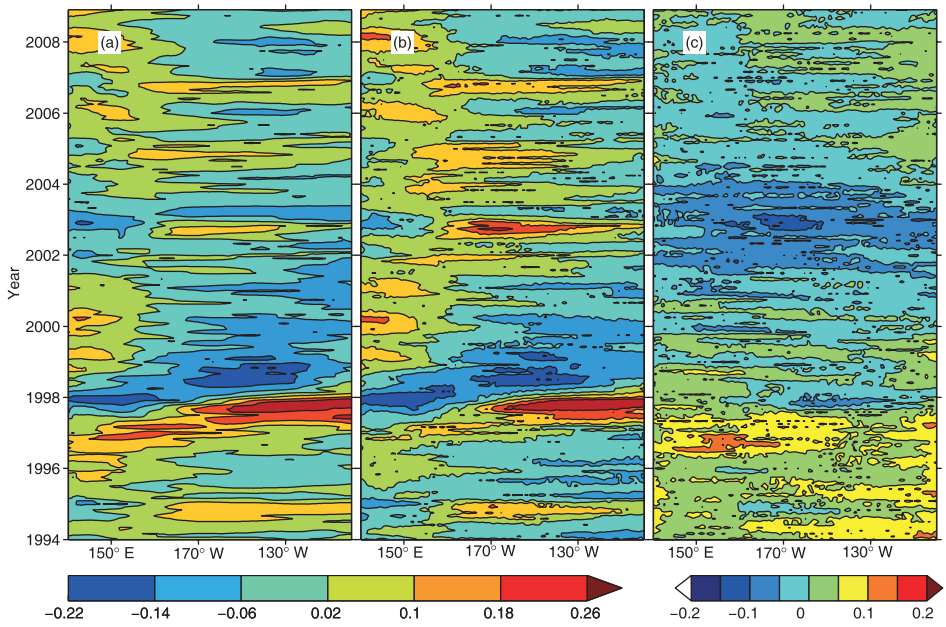

Fig. 11. Hovmoeller plots of SLAs (units: m) averaged for 2°S–2°N of (a) CORA; (b) AVISO altimetry data; and (c) CORA minus AVISO altimetry data.

tionship, especially when salinity observations are very sparse.

Acknowledgements. This research was sponsored by the National Basic Research Program (Grant No. 2013 CB430304), National Natural Science Foundation of China (Grant Nos. 41030854, 41106005, 41176003, and 41206178), and National High-Tech R&D Program of China (Grant No. 2013AA09A505). The temperature and salinity *in-situ* profiles were obtained from WOD09, maintained by NODC, USA, the GTSPP project and Argo global data center (Coriolis Data Center, ftp://ftp.ifremer.fr). The multi-satellite altimeter SLA data were from http://www.jason.oceanobs.com, the TAO mooring current data from http://www.pmel.noaa.gov/tao, the Reynolds SST dataset ftp://eclipse.ncdc.noaa.gov/pub/OI-daily/NetCDF/, from the NCEP reanalysis from ftp://ftp.cdc.noaa.gov/pub/datasets/necp.reanalysis2, the CCMP ocean surface wind data from PO. DAAC (http://podaac.jpl.nasa.gov/DATA_CATALOG/ccmpinfo.html), and the SODA reanalysis from http://dsrs.atmos.umd.edu.

REFERENCES

Atlas, R., R. N. Hoffman, J. Ardizzone, S. M. Leidner, J. C. Jusem, D. K. Smith, and D. Gombos, 2011: A cross-calibrated, multiplatform ocean surface wind velocity product for meteorological and oceanographic applications. *Bull. Amer. Meteor. Soc.*, **92**(2), 157–174.

Carton, J. A., and B. S. Giese, 2008: A reanalysis of ocean climate using simple ocean data assimilation (SODA). *Mon. Wea. Rev.*, **136**, 2999–3017.

Carton, J. A., G. Chepurin, and X. Cao, 2000a: A simple ocean data assimilation analysis of the global upper ocean 1950–95. Part I: Methodology. *J. Phys. Oceanogr.*, **30**, 294–309.

Carton, J. A., G. Chepurin, and X. Cao, 2000b: A simple ocean data assimilation analysis of the global upper ocean 1950–95. Part II: Results. *J. Phys. Oceanogr.*, **30**, 311–326.

Derber, J., and A. Rosati, 1989: A global oceanic data assimilation system. *J. Phys. Oceanogr.*, **19**, 1333–1347.

Dong, S. F., S. Garzoli, M. Baringer, C. Meinen, G. Goni, 2009: Interannual variations in the Atlantic meridional overturning circulation and its relationship with the net northward heat transport in the South Atlantic. *Geophys. Res. Lett.*, **36**, L20606, doi: 10.1029/2009GL039356.

Dursku, S. M., S. M. Glenn, and D. B. Haidvogel, 2004: Vertical mixing schemes in the coastal ocean: Comparison of the level 2.5 Mellor-Yamada scheme with an enhanced version of the K profile parameterization. *J. Geophys. Res.*, **109**(C01015), 1029–1051.

Han, G. J and Coauthors 2011: A regional ocean reanalysis system for coastal waters of china and adjacent seas. *Adv. Atmos. Sci.*, **28**(3), 682–690, doi: 10.1007/s00376-010-9184-2.

He, Z. J., G. J. Han, W. Li, D. Li, X. F. Zhang, X. D. Wang, and X. R. Wu, 2010: Experiments on assimilating of satellite data in the China seas and adjacent

seas. *Periodical of Ocean University of China*, **40**(9), 1–7. (in Chinese)

Large, W. G., J. C. McWilliams, and S. C. Doney, 1994: Oceanic vertical mixing: A review and a model with a nonlocal boundary layer parameterization. *Rev. Geophys.*, **32**, 363–403.

Li, W., Y. F. Xie, Z. J. He, K. X. Liu, G. J. Han, J. R. Ma, and D. Li, 2008: Application of the multi-grid data assimilation scheme to the China Seas' temperature forecast. *J. Atmos. Oceanic. Technol.*, **25**(11), 2106–2116.

Li, W., Y. F. Xie, S. M. Deng, and Q. Wang, 2010: Application of the multigrid method to the two-dimensional doppler radar radial velocity data assimilation. *J. Atmos. Oceanic. Technol.*, **27**(2), 319–332.

Marshall, J., C. Hill, L. Perelman, and A. Adcroft, 1997: Hydrostatic, quasi-hydrostatic, and nonhydrostatic ocean modelling. *J. Geophys. Res.*, **102**(C3), 5733–5753.

Reynolds, R. W., T. M. Smith, C. Liu, D. B. Chelton, K. S. Casey, and M. G. Schlax, 2007: Daily high-resolution blended analyses for sea surface temperature. *J. Climate*, **20**(22), 5473–5496.

Shu, Y. Q., J. Zhu, D. X. Wang, C. X. Yan, and X. J. Xiao, 2009: Performance of four sea surface temperature assimilation schemes in the South China Sea. *Continental Shelf Research*, **29**, 1489–1501.

Shu, Y. Q., J. Zhu, and D. X. Wang, 2011: Assimilating remote sensing and in situ observations into a coastal model of northern South China Sea using ensemble Kalman filter. *Continental Shelf Research*, **31**, S24–S36.

Stammer, D., and E. P. Chassignet, 2000: Ocean state estimation and prediction in support of oceanographic research. *Oceanography*, **13**, 51–56.

Troccoli, A., and Coauthors, 2002: Salinity adjustments in the presence of temperature data assimilation. *Mon. Wea. Rev.*, **130**, 89–102.

Wang, D. X., Y. H. Qin, X. J. Xiao, Z. Q. Zhang, and F. M. Wu, 2012a: Preliminary results of a new global ocean reanalysis. *Chinese Science Bulletin*, **57**, 3509–3517.

Wang, D. X., Y. H. Qin, X. J. Xiao, Z. Q. Zhang, and X. Y. Wu, 2012b: El Niño and El Niño Modoki variability based on a new ocean reanalysis. *Ocean Dynamics*, **62**, 1311–1322.

Wong, A. P. S., G. C. Johnson, and W. B. Owens, 2003: Delayed-mode calibration of autonomous CTD profiling float salinity data by S–θ climatology. *J. Atmos. Oceanic Technol.*, **20**, 308–318.

Xiao, X. J., D. X. Wang, and J. J. Xu, 2006: The assimilation experiment in the southwestern South China Sea in summer 2000. *Chinese Science Bulletin*, **51**, doi: 10.1007/s11434-006-9031-4.

Xiao, X. J., D. X. Wang, C. X. Yan, and J. Zhu, 2008: Evaluation of a 3DVAR system for the South China Sea. *Progress in Natural Science*, **18**, 547–554.

Xie, Y., S. Koch, J. Mcginley, S. Albers, P. E. Bieringer, M. Wolfson, and M. Chan, 2011: A space-time multiscale analysis system: a sequential variational analysis approach. *Mon. Wea. Rev.*, **139**, 1224–1240.

Yan, C. X., J. Zhu, and G. Q. Zhou, 2004: The roles of vertical correlation of the background covariance and T-S relation in estimation temperature and salinity profiles from surface dynamic height. *J. Geophys. Res.*, **109**, doi: 10. 1029/2003JC002224.

Yelland, M., and P. K. Taylor, 1996: Wind stress measurements from the open ocean. *J. Phys. Oceanogr.*, **26**, 541–558.

Zhu, J., and C. X. Yan, 2006: Nonlinear balance constraint in 3DVAR. *Sci. China* (*D*), **49**, 331–336.

Zhu, J., G. Q. Zhou, C. X. Yan, and X. B. You, 2006: A three-dimensional variational ocean data assimilation system: Scheme and preliminary results. *Sci. China* (*D*), **49**(12), 1212–1222.